ChemPubSoc Europe

DOI: 10.1002/chem.201600892

CHEMISTRY A European Journal Full Paper

Peptide Synthesis

Solid-Phase Synthesis and Characterization of N-Terminally Elongated Aβ$_{-3-x}$-Peptides

Isaak Beyer[+],[a] Nasrollah Rezaei-Ghaleh[+],[b, c] Hans-Wolfgang Klafki,[d] Olaf Jahn,[e, f] Ute Haußmann,[g] Jens Wiltfang,*[c, d] Markus Zweckstetter,*[b, c, f] and Hans-Joachim Knölker*[a]

Abstract: In addition to the prototypic amyloid-β (Aβ) peptides Aβ$_{1-40}$ and Aβ$_{1-42}$, several Aβ variants differing in their amino and carboxy termini have been described. Synthetic availability of an Aβ variant is often the key to study its role under physiological or pathological conditions. Herein, we report a protocol for the efficient solid-phase peptide synthesis of the N-terminally elongated Aβ-peptides Aβ$_{-3-38}$, Aβ$_{-3-40}$, and Aβ$_{-3-42}$. Biophysical characterization by NMR spectroscopy, CD spectroscopy, an aggregation assay, and electron microscopy revealed that all three peptides were prone to aggregation into amyloid fibrils. Immunoprecipitation, followed by mass spectrometry, indicated that Aβ$_{-3-38}$ and Aβ$_{-3-40}$ are generated by transfected cells even in the presence of a tripartite β-site amyloid precursor protein cleaving enzyme 1 (BACE1) inhibitor. The elongated Aβ peptides starting at Val(−3) can be separated from N-terminally-truncated Aβ forms by high-resolution isoelectric-focusing techniques, despite virtually identical isoelectric points. The synthetic Aβ variants and the methods presented here are providing tools to advance our understanding of the potential roles of N-terminally elongated Aβ variants in Alzheimer's disease.

Introduction

Brain deposition of amyloid-β (Aβ) peptides into neuritic plaques is one of the classical neuropathological hallmarks of Alzheimer's disease (AD).[1] Aβ peptides are generated under physiological conditions by consecutive proteolytic cleavages of the amyloid precursor protein (APP) by so-called β- and γ-secretases.[2] A well-known "non-amyloidogenic" APP processing pathway involves cleavage within the Aβ-sequence by α-secretase.[3,4] Recently, further cellular APP processing pathways involving η- and δ-secretases, both cleaving full length APP N-terminally to the β-secretase cleavage site, were reported.[5,6]

A considerable number of Aβ variants differing in the exact length of their amino and carboxy termini have been identified in amyloid plaques,[7] in blood plasma,[8] and in the cerebrospinal fluid (CSF).[9] In particular, Aβ peptides ending at Ala(42) (Aβ$_{42}$)[10,11] and N-terminally truncated Aβ peptides starting with Glu(3), post-translationally cyclized into pyroglutamic acid (N3pE),[12,13] or Phe(4) are highly abundant in the parenchymal amyloid plaques in AD brain.[1] Well documented and widely accepted biomarkers of cerebral Aβ accumulation, which have been incorporated into updated recommendations on diagnostic guidelines for Alzheimer's disease, are increased tracer signals on amyloid positron emission tomography (PET) imaging and low levels of soluble Aβ$_{42}$ in the CSF.[14] Recently, the concentration ratio of the Aβ peptides APP669–711/Aβ$_{1-42}$ in blood plasma, as measured by immunoprecipitation followed by mass spectrometry, was reported to be strongly and positively correlated with amyloid PET.[15] A validated and reliable biochemical AD-surrogate biomarker in blood would be highly

[a] I. Beyer,[+] Prof. Dr. H.-J. Knölker
Department Chemie, Technische Universität Dresden
Bergstrasse 66, 01069 Dresden (Germany)
Fax: (+49) 351 463 37030
E-mail: hans-joachim.knoelker@tu-dresden.de

[b] Dr. N. Rezaei-Ghaleh,[+] Prof. Dr. M. Zweckstetter
Max Planck Institute for Biophysical Chemistry
Am Fassberg 11, 37077 Göttingen (Germany)

[c] Dr. N. Rezaei-Ghaleh,[+] Prof. Dr. J. Wiltfang, Prof. Dr. M. Zweckstetter
German Center for Neurodegenerative Diseases (DZNE)
Von-Siebold-Str. 3a, 37075 Göttingen (Germany)
E-mail: Markus.Zweckstetter@dzne.de

[d] Dr. H.-W. Klafki, Prof. Dr. J. Wiltfang
Department of Psychiatry and Psychotherapy
University Medical Center Göttingen, Georg-August-Universität
37075 Göttingen (Germany)
E-mail: jens.wiltfang@med.uni-goettingen.de

[e] Dr. O. Jahn
Max Planck Institute for Experimental Medicine
Proteomics Group, 37075 Göttingen (Germany)

[f] Dr. O. Jahn, Prof. Dr. M. Zweckstetter
Center for Nanoscale Microscopy and Molecular Physiology of the Brain,
University Medical Center Göttingen
University of Göttingen, Humboldtallee 23, 37073 Göttingen (Germany)

[g] Dr. U. Haußmann
University of Duisburg-Essen, 45141 Essen (Germany)

[+] These authors contributed equally to this work.

Supporting information for this article can be found under http://dx.doi.org/10.1002/chem.201600892.

Table 1. Amino acid sequence and yields of the N-terminally elongated Aβ peptides $Aβ_{-3-38}$, $Aβ_{-3-40}$, and $Aβ_{-3-42}$ (**1**–**3**).

	Aβ	Sequence	Isolated yield [%][a]
1	−3–38	H-VKMD^{1}AEFRHDSGYEVHHQKLVFFAEDVGSNKGAIIGLMVGG^{38}-OH	5.7
2	−3–40	H-VKMD^{1}AEFRHDSGYEVHHQKLVFFAEDVGSNKGAIIGLMVGGVV^{40}-OH	4.7
3	−3–42	H-VKMD^{1}AEFRHDSGYEVHHQKLVFFAEDVGSNKGAIIGLMVGGVVIA^{42}-OH	3.3

[a] Yields after purification of the crude products by preparative HPLC.

advantageous for clinical routine, in particular since blood is much easier accessible than the CSF. The peptide APP669–711 (APP770 numbering) refers to an $Aβ_{40}$ peptide starting 3 residues upstream of the "classical" Aβ sequence, that begins with Asp(1). We thus refer to this peptide as $Aβ_{-3-40}$. The source of $Aβ_{-3-40}$ in blood is currently unknown, neither is its role under physiological or pathological conditions. In cell culture supernatants of the Chinese hamster ovary cell line 7PA2, transfected with mutant APP751 (Val–Phe 717), $Aβ_{-3-40}$ was reported to be increased on inhibition of the β-site APP-cleaving enzyme 1 (BACE1), suggesting that it results from an APP-processing pathway independent of BACE1.[16] Herein, we describe the solid-phase synthesis of the three N-terminally elongated Aβ peptides $Aβ_{-3-38}$ (**1**), $Aβ_{-3-40}$ (**2**), and $Aβ_{-3-42}$ (**3**) (Table 1). We also present a comprehensive biophysical characterization of the N-terminally elongated peptides addressing peptide conformations and their aggregation into β-sheet-enriched amyloid fibrils in vitro. Moreover, we have identified $Aβ_{-3-40}$ (**2**) to represent one of the BACE-inhibitor-resistant Aβ peptides produced from SH-SY5Y cells transfected with wild-type human APP.

Results and Discussion

Several Aβ variants have already been synthesized by various techniques including solid-phase peptide synthesis (SPPS).[17,18] The synthesis of Aβ peptides, elongated by three residues at the N-terminus, was achieved by automated solid-phase peptide synthesis on an ABI 433A peptide synthesizer. Attempts to obtain the Aβ peptides **1**–**3** using a Wang resin on polystyrene as a solid support, the standard FastMoc protocol from ABI, and the *O*-acyl-isopeptide method failed.[17c–e] However, when using a Wang resin on polyethylene glycol as a solid support (0.1 mmol scale)[17b] in combination with a 10-fold excess of Fmoc-protected amino acids (1 mmol), extended coupling times (35 min or 50 min),[17b,20] and a twofold coupling for the amino acids Ser(26) and Ala(30), the Aβ peptides **1**–**3** were obtained as major products (see Experimental Section). After purification by preparative HPLC, the Aβ peptides **1**–**3** were isolated in good yields (Table 1) and high purities (Table 2). The characterization of **1**–**3** was achieved by high-resolution ESI-MS (Table 2, Supporting Information).

For $Aβ_{-3-38}$ (**1**) and $Aβ_{-3-40}$ (**2**) the isolation after SPPS and purification by preparative HPLC was achieved without any difficulty in a standard manner. However, the behavior of $Aβ_{-3-42}$ (**3**) was very different. Some of the $Aβ_{-3-42}$ (**3**) precipitated already during cleavage of the crude peptide from the PEG resin, indicating that more of the cleavage reagent (TFA/1,2-ethanedithiol/H_2O/iPr_3Si-H, 95:2:2:1) was required in order to remove the peptide completely from the resin. Moreover, for HPLC the standard polar gradient proved to be unsuitable. With water as major component of the mobile phase, $Aβ_{-3-42}$ (**3**) formed undefined oligomers that were eluting from the column over a long period of time. Using acetonitrile as major component in the HPLC solvent mixture for the purification process, $Aβ_{-3-42}$ (**3**) eluted from the column as a single peak after about 3 min (Table 2). This procedure provided the N-terminally elongated Aβ peptides **1**–**3** in quantities of 15–30 mg (see Experimental Section). Since the Aβ peptides can misfold and give rise to aggregates leading to oligomers and fibrils, they are considered as peptides which are difficult to synthesize.[19] Therefore, the present synthesis of the Aβ peptides **1**–**3** is remarkable with respect to scale and purity.

Table 2. Analytical data for the Aβ peptides **1**–**3**.

	Retention time [min][a]	Purity [%][b]	*M* [calcd][c]	*M* [found][d]
1	20.6[e]	98.0	4487.2155	4487.2167
2	18.4[e]	97.4	4685.3523	4685.3490
3	2.92[f]	99.9	4869.4735	4869.4698

[a] Retention time on analytical HPLC; column: Vydac 208TP104 (reversed phase C_8, 4.6×250 mm); flow rate: 1.0 mL min^{-1}; eluent A: H_2O with 0.1% TFA; eluent B: MeCN with 0.1% TFA. [b] Purity based on analysis by an evaporative light-scattering detector. [c] Calculated monoisotopic mass. [d] Monoisotopic mass reconstructed by deconvolution of the ESI mass spectra. [e] Gradient from 20% to 50% of eluent B in 30 min. [f] Gradient from 60% to 90% of eluent B in 30 min.

Several N-terminally elongated peptides including $Aβ_{-3-38}$ (APP669–709), $Aβ_{-3-39}$ (APP669–710) and $Aβ_{-3-40}$ (APP669–711) have been identified in human EDTA-blood plasma.[15] Furthermore, the ratio of $Aβ_{-3-40}$ to $Aβ_{1-42}$ (APP669–711/Aβ1–42) was proposed as a novel peripheral surrogate biomarker of amyloid deposition in the brain of AD patients.[15b] So far, nothing is known about the structure of the $Aβ_{-3-40}$ peptide (**2**) and its potential to form insoluble aggregates. Having the N-terminally elongated Aβ peptides **1**–**3** available by synthesis, we first sought to obtain insight into the overall structure of $Aβ_{-3-40}$ (**2**) in solution by pulse-field gradient (PFG)-NMR experiments, which quantify the diffusion of molecules and thus allow quantification of their hydrodynamic radius (Table 3). Application of PFG-NMR measurements to 70 μM of freshly dissolved $Aβ_{-3-40}$ (**2**) resulted in a translational diffusion coefficient of 5.9×10^{-7} cm^2 s^{-1}.[21] On the basis of this diffusion coefficient and the Stokes–Einstein equation, a hydrodynamic radius R_h of 1.91 nm was calculated for $Aβ_{-3-40}$ (**2**). This hydrodynamic radius is consistent with an elongated, disordered peptide of

Table 3. Translational diffusion coefficients and hydrodynamic radii of Aβ peptide variants obtained through PFG-NMR diffusion measurements.

	D_t [10^{-7} cm^2 s^{-1}] (at 5 °C)[c,d]	R_h [nm][d]
dioxane[a]	53.2 ± 0.3	0.212
DSS[b]	27.3 ± 0.4	0.41 ± 0.01
$A\beta_{-3-38}$ (**1**)	6.3 ± 0.2	1.79 ± 0.07
$A\beta_{-3-40}$ (**2**)	5.9 ± 0.3	1.91 ± 0.08
$A\beta_{-3-42}$ (**3**)	7.0 ± 0.2	1.60 ± 0.04
$A\beta_{1-42}$	6.6 ± 0.1	1.71 ± 0.03

[a] The hydrodynamic radius of dioxane was used for viscosity correction. [b] DSS = 4,4-Dimethyl-4-silapentane-1-sulfonic acid. [c] Translational diffusion coefficients were obtained after gradient calibration as described previously.[21] [d] The errors represent 95% confidence intervals.

43 amino acids.[22] Next, we investigated the two N-terminally elongated peptides, which end either at residue 38 ($A\beta_{-3-38}$) (**1**) or 42 ($A\beta_{-3-42}$) (**3**). Determination of the translational diffusion coefficients followed by calculation of R_h, resulted in values of 1.79 and 1.60 nm for $A\beta_{-3-38}$ (**1**) and $A\beta_{-3-42}$ (**3**), respectively. Despite the longer sequence, the R_h of $A\beta_{-3-42}$ (**3**) was slightly smaller than that of $A\beta_{-3-38}$ (**1**) and $A\beta_{-3-40}$ (**2**). This result suggests that $A\beta_{-3-42}$ (**3**) is more compact than the peptides **1** and **2**.

It is known that $A\beta_{1-40}$ and $A\beta_{1-42}$ monomers in aqueous solution are mainly unstructured,[23,24] but exhibit a tendency to adopt β-hairpin conformations.[24,25] To gain insight into the monomeric structure of the N-terminally elongated Aβ peptides at single residue level, 2D homonuclear proton NMR spectra were measured for freshly prepared $A\beta_{-3-38}$ (**1**), $A\beta_{-3-40}$ (**2**), and $A\beta_{-3-42}$ (**3**) samples (ca. 70 μM, pH 7.4 buffered with 20 mM sodium phosphate). The sequence-specific proton-resonance assignments of all three peptides were obtained through the analysis of two-dimensional TOCSY and NOESY spectra. We then compared the TOCSY spectra of the three peptides **1–3** (Figure 1). These peptides, which all start at position −3 and only differ at the C-terminus, show a nearly complete overlay of their TOCSY spectra, with differences being restricted to the immediate C-terminal regions (Figure 1B). In contrast, the chemical shifts of $A\beta_{-3-40}$ (**2**) and $A\beta_{1-40}$ revealed some interesting differences beyond the presence of the four additional peaks, which correspond to Lys(−2), Met(−1), Asp(1), and Ala(2) (Figure 1A). In particular, the cross peaks of residues Glu(3), Phe(4), Arg(5), and to a lesser extent Asp(7), Gly(9), and Tyr(10) showed perturbations in their HN chemical shifts. Moreover, the chemical-shift deviations were not limited to the N-terminal region of Aβ, but also included residue Ser(26), which points to a long-range effect of the N-terminal elongation. Taken together, the NMR data demonstrate that N-terminally elongated Aβ peptides are disordered in solution and that N-terminal elongation influences the backbone conformation of Aβ particularly in, but not limited to, its N-terminal region.

The N-terminal region of Aβ peptides is highly important for its aggregation and toxicity.[26–28] We therefore decided to investigate the impact of N-terminal elongation on the aggregation behavior of Aβ peptides using a set of biophysical techniques. First, we performed an NMR-based monomer-consumption assay to quantify the time-dependent conversion of Aβ monomers to NMR-invisible aggregates. The 1D proton NMR spectra of Aβ samples were measured before and after

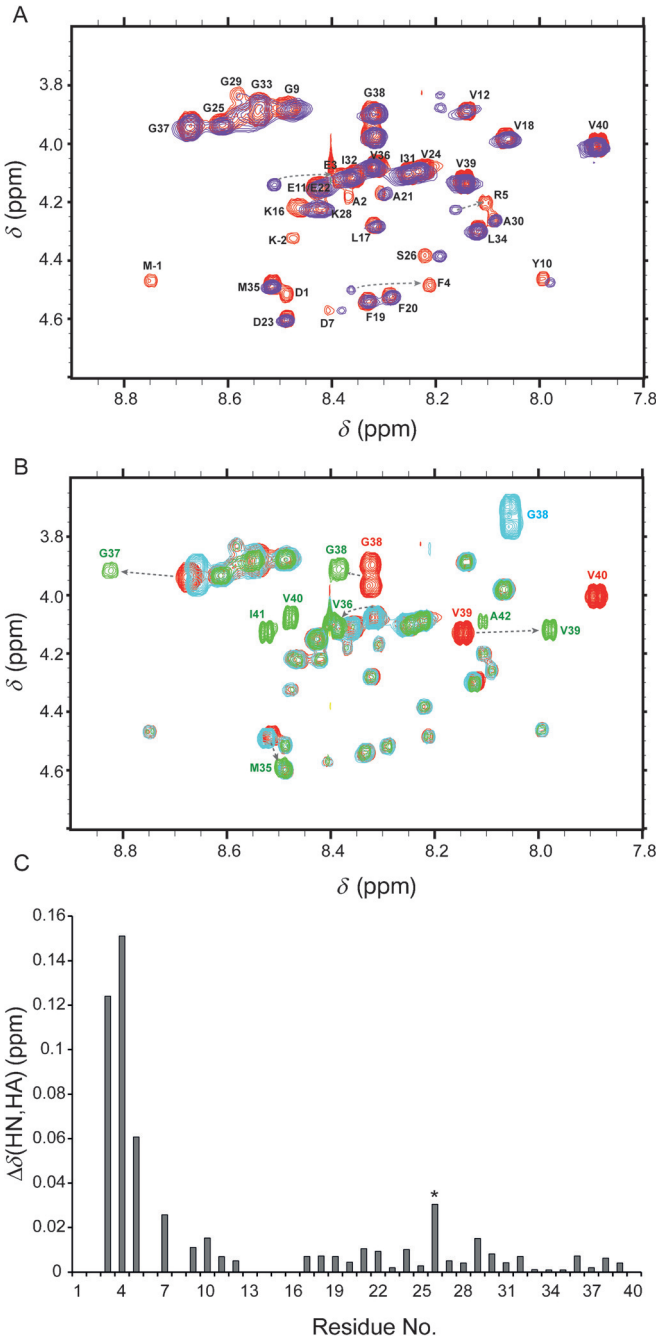

Figure 1. Effects of N-terminal elongation on the structure of Aβ peptides as revealed by 2D proton-proton NMR spectroscopy. A) Superimposed TOCSY spectra of $A\beta_{1-40}$ (purple) and $A\beta_{-3-40}$ (**2**) (red) along with cross-peak assignments. Some additional peaks are observed in the spectrum of $A\beta_{-3-40}$ (**2**) (M-1, K-2, D1, A2). Peaks with strong displacement are highlighted by arrows (E3, F4, R5). B) Superposition of the TOCSY spectra of $A\beta_{-3-38}$ (**1**) (cyan), $A\beta_{-3-40}$ (**2**) (red), and $A\beta_{-3-42}$ (**3**) (green) show a nearly perfect fit except in their differing C-terminal region. C) Combined HN and HA chemical-shift difference between $A\beta_{1-40}$ and $A\beta_{-3-40}$ (**2**) indicate local conformational changes in the N-terminal region as well as a long-range effect on residue Ser(26) (highlighted by asterisk).

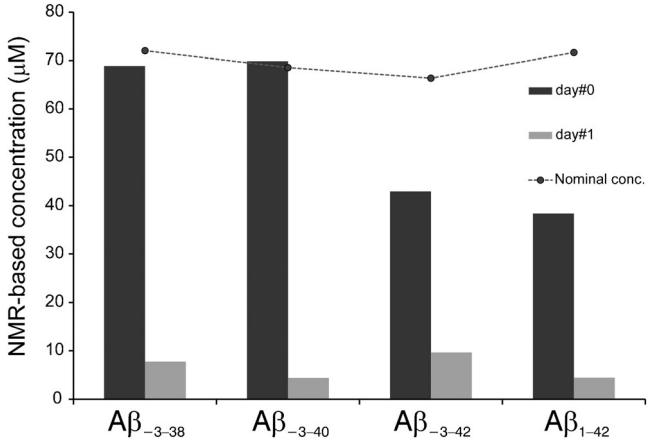

Figure 2. Aβ peptide monomer consumption during aggregation as evaluated by NMR spectroscopy. The nominal Aβ peptide concentration is displayed by filled circles. After 1 day of aggregation, the monomer concentration, determined by NMR spectroscopy, significantly decreased in all Aβ peptide variants of this study. The relative errors in peptide concentration estimated from duplicate NMR measurements are smaller than 1%.

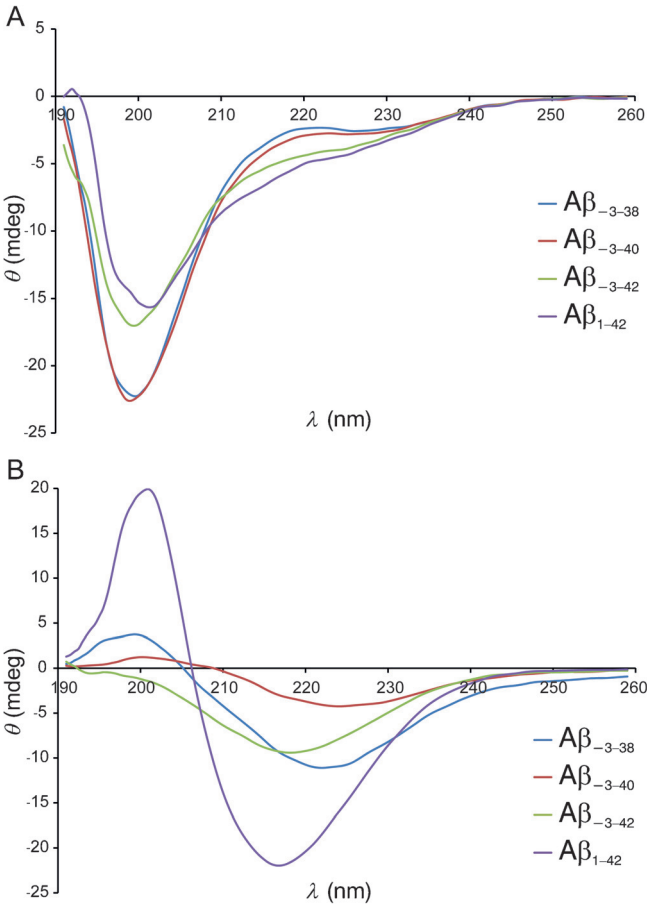

Figure 3. UV-CD spectra of Aβ peptides A) before and B) after aggregation. A) The freshly prepared Aβ peptide solutions showed predominantly coil-like structures with a negative band around 200 nm. B) After aggregation, a prominent coil-to-beta transition occurred in all studied Aβ peptide variants. The CD intensity difference in B) was partially caused by precipitation of large Aβ peptide aggregates during the experiments.

24 h of incubation in aggregation-prone conditions (37 °C, gentle stirring). The concentration of monomeric Aβ was estimated from the NMR signal intensity using DSS (4,4-dimethyl-4-silapentane-1-sulfonic acid) as internal reference. Immediately after dissolving and before incubation, the monomeric concentrations of $Aβ_{-3–38}$ (**1**) and $Aβ_{-3–40}$ (**2**), as estimated by NMR spectroscopy, were very close to their nominal concentration, indicating that they were almost fully solubilized (Figure 2). On the other hand, the initial monomeric concentration of $Aβ_{-3–42}$ (**3**) was approximately only 60% of its nominal concentration, reflecting its limited solubility. After 24 h of incubation, the monomer concentrations of $Aβ_{-3–38}$ (**1**), $Aβ_{-3–40}$ (**2**), $Aβ_{-3–42}$ (**3**), and $Aβ_{1–42}$ decreased to 11, 6, 15, and 6% of the initial nominal concentrations, respectively (Figure 2). Thus, the N-terminally elongated Aβ peptides (**1**–**3**) rapidly assemble into high-molecular-weight aggregates. Further comparison of the data for $Aβ_{-3–42}$ (**3**) and $Aβ_{1–42}$ showed that N-terminal elongation resulted in a decreased Aβ peptide monomer loss.

Next, we monitored if the secondary structures of the N-terminally elongated Aβ peptides (**1**–**3**) were altered during aggregation. To this end, we used UV circular dichroism (Figure 3A). Before aggregation, $Aβ_{-3–38}$ (**1**), $Aβ_{-3–40}$ (**2**), $Aβ_{-3–42}$ (**3**), and $Aβ_{1–42}$ showed CD spectra with negative minima around 200 nm, which are characteristic for disordered polypeptide conformations. In agreement with their incomplete solubilization, evidenced by NMR spectroscopy (see above), the CD spectra of $Aβ_{-3–42}$ (**3**) and $Aβ_{1–42}$ had less negative ellipticities at 200 nm. In addition, larger negative ellipticities were observed around 220 nm, indicating the copresence of β-sheet-rich aggregates in these samples. After 24 h of aggregation, all four Aβ peptide variants exhibited structural conversion from random-coil to β-sheet (Figure 3B). The spectra of the aggregated $Aβ_{1–42}$, and to a lesser degree $Aβ_{-3–42}$ (**3**), contained strong negative peaks around 217–219 nm, indicative of extended β-sheet segments. In contrast, the CD spectra of aggregated $Aβ_{-3–38}$ (**1**), and in particular $Aβ_{-3–40}$ (**2**), showed significant red shifts of this negative peak to about 222–224 nm, suggesting that the aggregated species of these two Aβ variants may contain some type-II β-turn structures.

CD spectroscopy showed that the N-terminally elongated Aβ peptides (**1**–**3**) aggregate into β-sheet-rich structures. To test if the formed aggregates are amyloid fibrils, we used the amyloid-specific dye thioflavin T (ThT). The fluorescence intensity of ThT is low when in solution or bound to less stable aggregation intermediates, but is very high when bound to amyloid fibrils.[29] All three N-terminally elongated Aβ peptide variants exhibited a high rate and amount of aggregation (Figure 4). After only one hour of incubation in aggregation-prone conditions a significant rise in ThT fluorescence emission intensity was observed for $Aβ_{-3–38}$ (**1**), $Aβ_{-3–40}$ (**2**), and $Aβ_{-3–42}$ (**3**). In case of $Aβ_{1–42}$, sizeable ThT fluorescence intensity was already present in freshly prepared samples, indicating the incomplete solubilization of preformed aggregates. To further investigate the ability of N-terminally elongated Aβ peptides to form amyloid fibrils, we examined the aggregated samples by electron microscopy. The peptide $Aβ_{-3–38}$ (**1**) formed fibrillar aggregates of various morphologies (Figure 5). The majority of

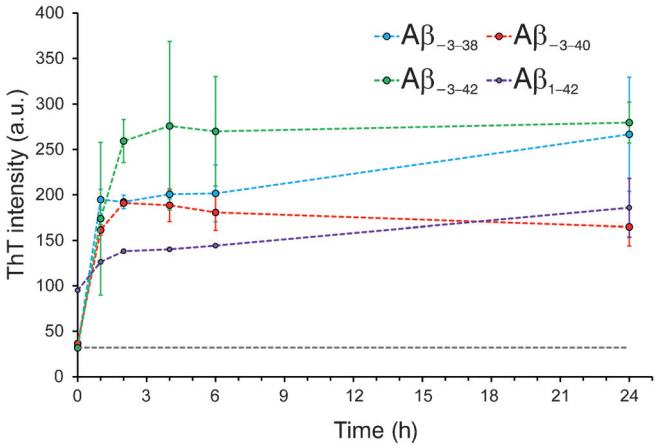

Figure 4. Fibrillar β-sheet-rich aggregation of Aβ peptides as followed by a thioflavin T (ThT) fluorescence assay. All three N-terminally elongated variants of Aβ peptides show a high rate and degree of ThT-reactive aggregation. Error bars represent one standard deviation of three measurements of separately aggregated samples.

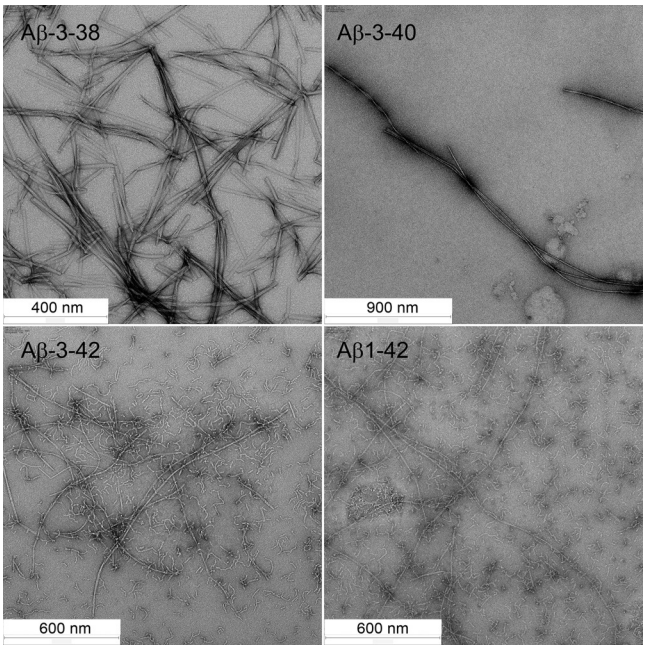

Figure 5. Electron microscopic images of the Aβ peptides **1–3** and $Aβ_{1–42}$ after 24 h incubation under aggregation-prone conditions (37 °C, gentle stirring) reveals their ability to form amyloid fibrils.

the aggregates were twisted pairs of long fibrils, while also some straight fibrils with or without lateral association were observed. In the $Aβ_{-3–40}$ (**2**) sample, fewer but longer fibrils were observed and they were predominantly twisted. In contrast, both $Aβ_{-3–42}$ (**3**) and $Aβ_{1–42}$ formed a mixture of short curved protofibrils and long twisted fibrils (Figure 5).

In order to evaluate the effect of N-terminal elongation on the kinetics of Aβ peptide fibrillar aggregation, we monitored the temporal development of ThT fluorescence in $Aβ_{x–40}$ and $Aβ_{x–42}$ peptide variants in a real-time manner. At a low peptide concentration of roughly 10 μM, incubation in mild aggregation conditions (room temperature, with agitation) resulted in a gradual increase in the ThT fluorescence intensities of all studied Aβ peptide variants (Figure 6). Table 4 summarizes the kinetic parameters obtained from the analysis of the ThT traces according to a logistic model.[26,30] The rate constants suggest that the N-terminal extension by three residues promoted the fibrillar aggregation of $Aβ_{40}$ and $Aβ_{42}$. It should, however, be noted that the fluorescence signal intensities of $Aβ_{-3–40}$ (**2**) frequently rose to the maximum detection limit of the fluorimeter, hence precluding a reliable quantitative analysis of its aggregation curves. Furthermore, the comparison of the aggregation kinetics between $Aβ_{1–42}$ and $Aβ_{-3–42}$ (**3**) was complicated by the presence of preformed aggregates in $Aβ_{1–42}$ samples as indicated by the relatively high ThT intensities at initial time points.

For further insight into the kinetics of Aβ peptide aggregation, we measured the rate of monomer loss during Aβ peptide aggregation within the NMR tube (37 °C, without agita-

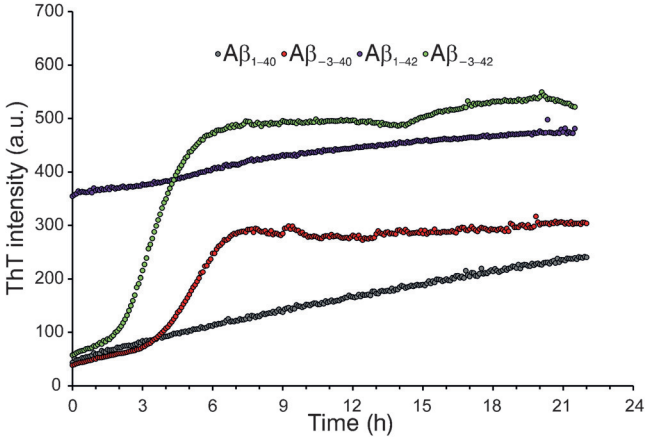

Figure 6. Real-time monitoring of thioflavin T (ThT) fluorescence during Aβ peptide incubation under aggregation-prone conditions (RT, 10 μM of Aβ peptide, gentle stirring). The N-terminally elongated variants of Aβ peptide (**2** and **3**) showed accelerated aggregation when compared to their corresponding $Aβ_{1–x}$ peptide analogues. Averages of three separate ThT traces are shown, except of $Aβ_{-3–40}$ (**2**) for which the ThT intensity in all but one trace quickly rose to the maximum detection limit of the fluorimeter.

Table 4. Kinetic parameters of Aβ peptide fibrillar aggregation obtained from analysis of the time-dependent increase in ThT fluorescence intensities.[a,b]

	F_0 [a.u.]	$t_{1/2}$ [h]	k [10^{-4} (a.u.)$^{-1}$ h^{-1}]	F_{lim} [a.u.]
$Aβ_{1–40}$	58 ± 16	8.6 ± 0.5	5.8 ± 1.3	267 ± 81
$Aβ_{-3–40}$	12 ± 2	4.3	25.9	293
$Aβ_{1–42}$	351 ± 13	–[c]	2.0 ± 0.3	503 ± 6
$Aβ_{-3–42}$	26 ± 1	3.1 ± 0.2	21.0 ± 10.8	509 ± 361

[a] F_0 and F_{lim} denote the initial and final fluorescence intensities; $t_{1/2}$ represents the time for Aβ peptide samples to reach half of their final ThT fluorescence intensities; k denotes a second-order rate constant governing the growth of ThT-reactive aggregates according to the equation: $dF/dt = kF(F_{lim}-F)$. [b] The errors represent the standard deviation of triplicate aggregation experiments. [c] For $Aβ_{1–42}$, $t_{1/2}$ was not determined since the initial fluorescence level (F_0) was already higher than half of the final level (F_{lim}).

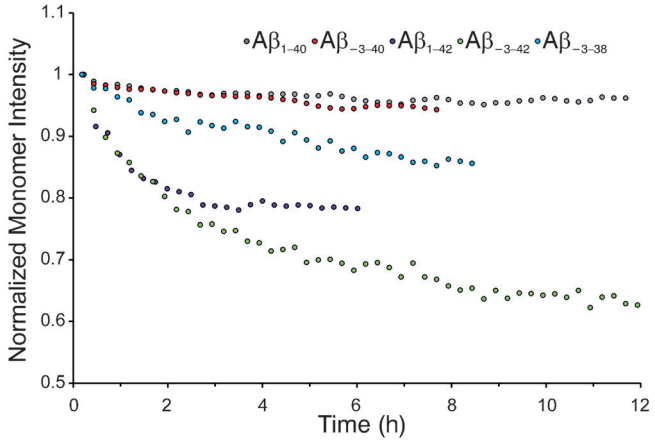

Figure 7. NMR-based monitoring of Aβ peptide-monomer consumption during aggregation induced by addition of aggregation seeds (37 °C, without agitation). The highest rates of Aβ peptide-monomer loss were observed in $Aβ_{x–42}$ peptide variants. No significant differences were observed between $Aβ_{1–42}$ and $Aβ_{–3–42}$ (**3**) or $Aβ_{1–40}$ and $Aβ_{–3–40}$ (**2**), especially in the initial parts of the monomer-consumption profiles.

tion). The aggregation reaction was initiated by addition of aggregation seeds, which were prepared from a mixture of amyloid aggregates from the Aβ peptide variants under investigation. The highest rates of monomer loss were observed for $Aβ_{–3–42}$ (**3**) and $Aβ_{1–42}$, followed by $Aβ_{–3–38}$ (**1**) and then by $Aβ_{–3–40}$ (**2**) and $Aβ_{1–40}$ (Figure 7). The comparison of the monomer-consumption profiles, especially in the initial parts, suggests that the N-terminal extension of Aβ peptides by three residues did not have any significant impact on the monomer-incorporation rates into previously formed aggregates. More rigorous kinetic experiments are, however, required before this conclusion can be confirmed.

Taken together, our data indicate that N-terminally elongated Aβ peptides (**1**–**3**) are disordered in solution and rapidly form β-sheet-rich fibrillar aggregates. From the comparison of $Aβ_{–3–x}$ with $Aβ_{1–x}$ we suggest that N-terminal elongation increases the propensity for aggregation, although the monomer incorporation rate to preformed aggregates does not seem to be significantly affected. This is in apparent contrast with a very recent study, in which the impact of N-terminal elongation, ranging from 5–40 amino acids in length, on the aggregation kinetics of recombinant variants of human $Aβ_{42}$ was investigated.[31] All of the N-terminally extended forms of $Aβ_{42}$ under investigation were shown to be able to form amyloid fibrils similar to those formed from $Aβ_{1–42}$, but with lower rates. The apparent discrepancy between these two studies may result from differences in experimental procedures such as solubilization of Aβ peptide prior to aggregation assays or the different lengths of the N-terminal extensions.

Six years ago, we reported that treatment of SH-SY5Y cells overexpressing wild type human APP with membrane-anchored tripartite BACE1 inhibitors reduced the overall cellular generation of Aβ peptide, but at the same time led to a relative increase in specific Aβ peptide variants displaying isoelectric points (pI) different from that of known Aβ peptides starting with Asp(1), that is, pI of approximately 5.4 according to 2D-Western blot analysis.[32] Mass spectrometry data indicated that the BACE1-inhibitor-resistant Aβ peptides comprise primarily N-truncated peptides starting with Arg(5), and have a pI of approximately 6.5 according to a novel capillary isoelectric-focusing (CIEF) immunoassay.[16,18,33–35] In addition, a minor fraction of BACE1-inhibitor-resistant Aβ peptides with a pI of approximately 6.0 was observed in supernatants of APP overexpressing SH-SY5Y cells (see Figure 2 in ref. [18]). Although $Aβ_{2–40}$/$Aβ_{3–40}$ were the most obvious candidates on the basis of their predicted isoelectric points, no evidence for the presence of such N-terminally truncated peptides was found using immunoprecipitation followed by mass spectrometry.[18] However, when considering the occurrence of N-terminally elongated Aβ variants we could now assign prominent signals to $Aβ_{–3–38}$ (**1**) and $Aβ_{–3–40}$ (**2**), and identify the latter as the main constituent of the minor fraction of BACE1-inhibitor-resistant Aβ peptides in the SH-SY5Y cell supernatant (Figure 8). Given that $Aβ_{2–40}$/$Aβ_{3–40}$ and $Aβ_{–3–40}$ (**2**) have a virtually identical predicted isoelectric point, the question arose whether these two Aβ classes can be separated by isoelectric-focusing techniques. The availability of synthetic $Aβ_{–3–40}$ (**2**) enabled us to directly compare the isoelectric points of $Aβ_{1–40}$, $Aβ_{2–40}$, and $Aβ_{–3–40}$ (**2**) by CIEF immunoassay (Figure 9). Most importantly, N-terminally elongated $Aβ_{–3–40}$ (**2**) can be resolved from N-terminally truncated $Aβ_{2–40}$ by isoelectric focusing due to subtle differences in net charge, providing a powerful tool to distinguish these two Aβ classes of biological and potentially pathological relevance.

Conclusion

We have developed an experimental procedure for the selective synthesis of the N-terminally elongated Aβ peptides $Aβ_{–3–38}$ (**1**), $Aβ_{–3–40}$ (**2**), and $Aβ_{–3–42}$ (**3**). In depth biophysical characterization indicated that all three elongated peptides are prone to aggregate into thioflavin T-positive amyloid fibrils. The cellular production from APP appears to occur independently of BACE1 activity in transfected SH-SY5Y cells. Given their occurrence in blood, the elongated Aβ peptides starting at Val(−3) may have relevance in the context of biomarker research. It is expected that the synthetic availability of these Aβ variants will advance the characterization of their potential roles under physiological or pathological conditions.

Experimental Section

Experimental procedure for the synthesis of the peptides 1–3: The Aβ peptides were prepared by Fmoc solid-phase peptide synthesis using an ABI 433A peptide synthesizer with UV-detector. Wang resin (NovaPEG Wang resin, 0.62 mmol g^{-1}, Novabiochem) was used as solid support, HBTU (2-(1*H*-benzotriazol-1-yl)-1,1,3,3-tetramethyluronium hexafluorophosphate) as activation agent, and piperidine for deprotection. The resin (Wang linker on polyethylene glycol, 0.1 mmol, Novabiochem) was manually loaded with the first amino acid using MSNT (1-(mesitylene-2-sulfonyl)-3-nitro-1,2,4-triazole) activation in order to prevent racemization.[36] For this purpose, the amino acid (20 equiv compared to the resin) was dissolved in CH_2Cl_2 (6 mL) and THF (2–3 mL) under an argon atmosphere. 1-Methylimidazole (15 equiv compared to the resin) and fi-

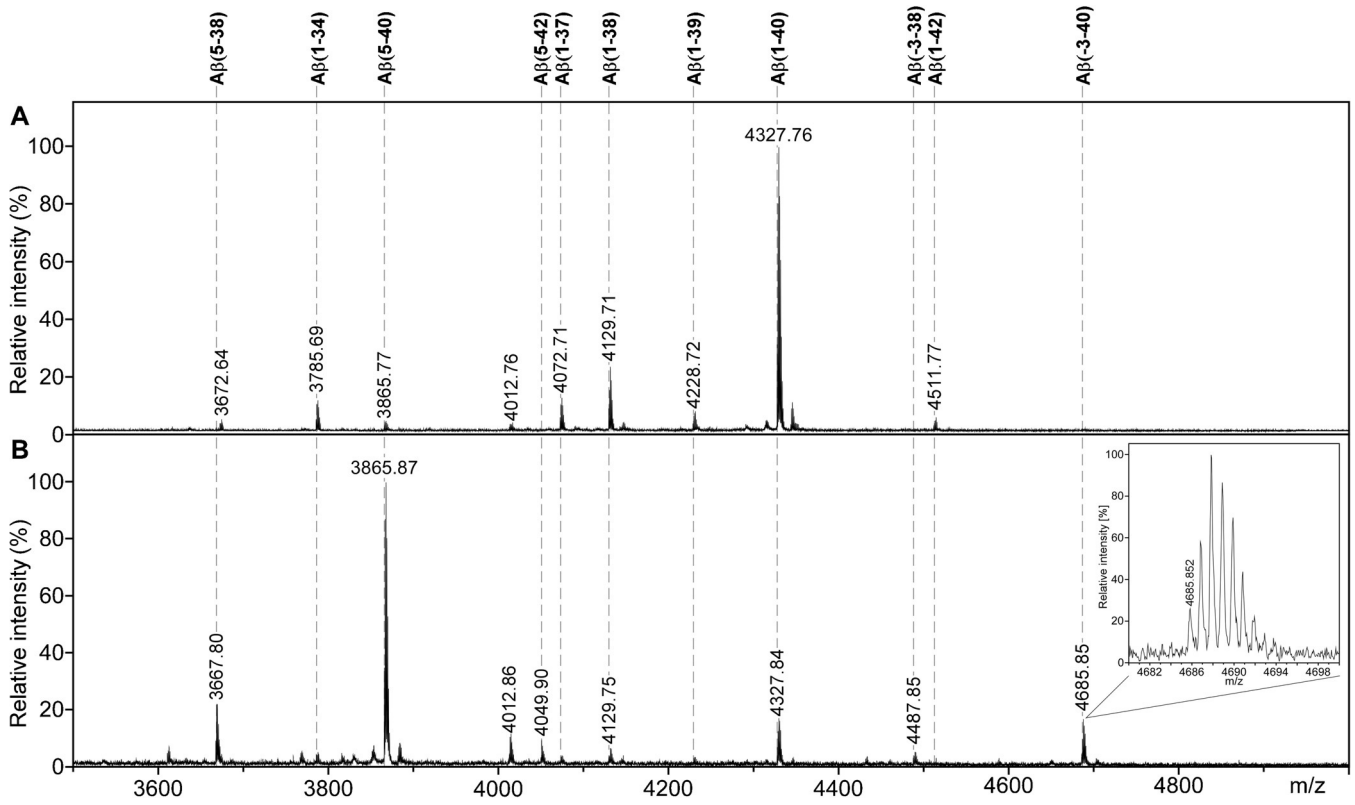

Figure 8. Mass-spectrometric identification of the Aβ peptides immunoprecipitated from cell-culture supernatants (SH-SY5Y cells overexpressing APPwt). A) Without BACE1 inhibition (0.1% DMSO as vehicle control). B) After treatment with 100 nM of a prototypic tripartite BACE1 inhibitor (compound **8g** in ref. [32a]) for 72 h. The Aβ peptides were immunoprecipitated from the conditioned media and analyzed by MALDI-MS. The inset shows the signal assigned to $Aβ_{-3-40}$ (**2**) in isotopic resolution, resulting in an accurate mass determination with only 108 ppm relative mass error (observed mass: $[M+H]^+_{obsd}$ = 4685.852; calcd. mass: $[M+H]^+_{calcd}$ = 4686.360).

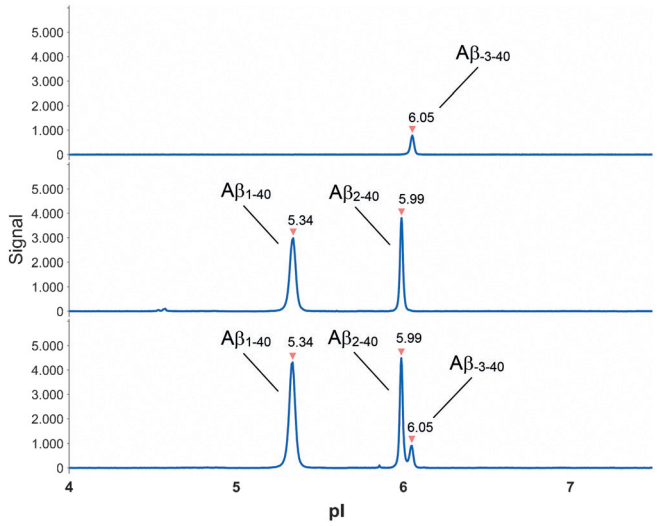

Figure 9. Comparison of the isoelectric points of the synthetic Aβ peptides $Aβ_{1-40}$, $Aβ_{2-40}$, and $Aβ_{-3-40}$ (**2**) by CIEF immunoassay. Starting from stock solutions in DMSO (1 mg mL^{-1}), the indicated Aβ peptides were prediluted with 20 mM bicine buffer (pH 7.6, 0.6% CHAPS) and analyzed by CIEF immunoassay as described previously.[18] The final concentrations of the Aβ peptides in the microcapillaries were 25 ng mL^{-1}, each. The immunological detection was achieved with monoclonal anti-Aβ antibody WO-2 (Millipore) in combination with biotinylated anti-mouse secondary antibody and streptavidin-coupled horseradish peroxidase (ProteinSimple). The electropherograms shown (baseline-corrected signals) were recorded with 30 s of exposure time.

nally MSNT (20 equiv compared to the resin) were added. This solution was added to the resin and stirred gently for 4 h. The mixture was transferred to the synthesizer, in which washing with CH_2Cl_2 and NMP was done. Then, acetylation of potentially free N-terminal groups at the resin was achieved by treatment with Ac_2O/iPr_2NEt in NMP. For the assembly of the peptide standard cycles were used with the exception of coupling times, which were increased from 15 min to 35 min and for some amino acids to 50 min (see below). For the synthesis of the peptides **1**–**3**, a twofold coupling was executed for Ser(26) and Ala(30). For the following amino acids extended coupling times of 50 min were applied: Ala(2), Glu(3), Phe(4), Arg(5), His(6), His(14), Gln(15), Lys(16), Leu(17), Val(18), Phe(19), Asp(23), Val(24), Gly(25), Ser(26) (with twofold coupling), Asn(27), Lys(28), Gly(29), Ala(30) (with twofold coupling), Ile(31), Ile(32), Gly(33), and Leu(34). After drying in vacuo, the peptide was cleaved from the resin with TFA/1,2-ethanedithiol/H_2O/iPr_3Si-H (95:2:2:1) at room temperature for 90 min. For $Aβ_{-3-42}$ (**3**), some of the peptide already precipitated on treatment with the cleavage reagent. The resin was removed by filtration and the peptide precipitated in MeO*t*Bu at −78 °C. The resulting white solid was collected by twofold centrifugation (the solution from first centrifugation was centrifuged a second time). The peptides were dissolved in H_2O with 0.1% TFA [for $Aβ_{-3-38}$ (**1**) and $Aβ_{-3-40}$ (**2**)] or hexafluoroisopropanol [for $Aβ_{-3-42}$ (**3**)] and subsequently purified by preparative HPLC (Varian PrepStar system, with Varian ProStar Model 320 UV and an evaporative light-scattering detector, ELS 1000, Polymer Laboratories; column: reversed phase C_8, 30× 250 mm, Vydac 208TP1030; flow rate: 20 mL min^{-1}) using H_2O with

0.1% TFA as eluent A and MeCN with 0.1% TFA as eluent B. For **1** and **2**, a gradient of 20% to 45% of eluent B over a period of 20 min afforded the peptides $A\beta_{-3-38}$ (**1**) (25.5 mg, 5.7 μmol, 5.7%) and $A\beta_{-3-40}$ (**2**) (22.1 mg, 4.7 μmol, 4.7%) as colorless amorphous solids after lyophilization. For **3**, a gradient of 60% to 90% of eluent B over a period of 20 min afforded the peptide $A\beta_{-3-42}$ (**3**) (16.3 mg, 3.3 μmol, 3.3%) as colorless amorphous solid after lyophilization. The purity of the peptides was confirmed by analytical HPLC (Agilent Model 1100 with G1315B UV-DAD and evaporative light-scattering detector, ELS 1000, Polymer Laboratories; column: reversed phase C_8, 4.6×250 mm, Vydac 208TP104; flow rate: 1.0 mL min^{-1}). Analysis was performed with H_2O with 0.1% TFA as eluent A and MeCN with 0.1% TFA as eluent B using a gradient of 20% to 50% of eluent B over a period of 30 min for $A\beta_{-3-38}$ (**1**) and $A\beta_{-3-40}$ (**2**). For $A\beta_{-3-42}$ (**3**), a gradient of 60% to 90% of eluent B was used over a period of 30 min. The identity of the products was confirmed by HR-MS (LTQ ORBITRAP XL, ThermoScientific) at a resolution of 60000 and a mass accuracy of 3 ppm (see Supporting Information).

Preparation of monomeric Aβ peptide samples: To dissociate preformed aggregates, the Aβ peptide powders were dissolved in 20 mM NaOH at 2 mg mL^{-1} peptide concentration and sonicated for 1 min.[37] After shaking for 30 min at 4 °C, the Aβ peptide solutions were exposed to ultracentrifugation (100000 g, 4 °C, 1 h). Subsequently, the supernatants were aliquoted, flash-frozen by liquid nitrogen, and stored at −80 °C until use. $A\beta_{1-42}$ was purchased from Peptide Specialty Laboratories (PSL) (Heidelberg, Germany) with a purity of more than 95%.

NMR spectroscopy: NMR measurements were performed on a 600 MHz Bruker spectrometer equipped with a cryogenic probe. NMR samples contained 0.25 mg mL^{-1} Aβ in 20 mM sodium phosphate (pH 7.4) plus 100 μM DSS (4,4-dimethyl-4-silapentane-1-sulfonic acid) for chemical shift referencing (0 ppm). 2D-^{1}H,^{1}H-TOCSY and NOESY spectra were obtained at 5 °C using mixing times of 60 and 80 ms for TOCSY and 200 and 300 ms for NOESY experiments. Peak assignments were made through standard homonuclear sequential-assignment strategy. The PFG-NMR experiments were measured at 5 °C as described previously.[21] Translational diffusion coefficients, obtained after gradient calibration,[21] were converted to hydrodynamic radii according to the Stokes–Einstein equation. The hydrodynamic radius of dioxane was used for the viscosity correction. For NMR-based monomer-consumption assays, 1D-^{1}H spectra were measured before and after 24 h of incubation under aggregation-prone conditions (37 °C, gentle stirring). The residual Aβ monomer levels were quantified on the basis of NMR-signal intensities in the methyl region using DSS as internal intensity reference. For real-time monitoring of Aβ monomer consumption, seeds of aggregation were added to 0.2 mg mL^{-1} Aβ samples (pH 7.4, buffered with 50 mM sodium phosphate, containing 50 mM NaCl and 500 μM DSS), then consecutive 1D-^{1}H spectra were measured at regular intervals, while the Aβ samples were incubated at 37 °C within the NMR spectrometer. The aggregation seeds were prepared after mixing the aggregated samples of $A\beta_{-3-38}$ (**1**), $A\beta_{1-40}$, $A\beta_{-3-40}$ (**2**), $A\beta_{1-42,}$ and $A\beta_{-3-42}$ (**3**), spinning down the fibrils (100000 g, 15 °C, 4 h), and sonication of resuspended Aβ fibrils for 30 min. The concentration ratio of seed to monomeric Aβ was smaller than 1%.

Circular dichroism: CD measurements were performed on a J-815 JASCO spectropolarimeter using a cuvette of 1 mm path length. Before and after 24 h of incubation under aggregation-prone conditions (37 °C, gentle stirring), the CD spectra of Aβ samples (0.2 mg mL^{-1}, pH 7.4 buffered with 20 mM sodium phosphate) were recorded at 20 °C between 190 and 260 nm.

Thioflavin T (ThT) aggregation assay: Aβ samples (0.2 mg mL^{-1}, pH 7.4 buffered with 20 mM sodium phosphate) were incubated under aggregation-prone conditions (37 °C, gentle stirring). Before and after the specified time points of incubation, the ThT assays were performed by mixing 10 μL aliquots of the Aβ samples with 2 mL ThT solution (5 μM, pH 8.0 buffered with 50 mM glycine). Fluorescence emission spectra were measured using a Cary Eclipse fluorescence spectrophotometer. The excitation wavelength was 446 nm and the ThT emission intensities were averaged between 478 and 488 nm. For the kinetic experiments presented in Figure 6, Aβ samples (0.04 mg mL^{-1} in PBS, containing 25 μM ThT) were incubated in mild aggregation conditions (RT, gentle stirring) and development of the ThT fluorescence was followed in a real-time manner with the excitation and emission wavelengths of 446 and 482 nm and slits of 10 nm. Aggregation experiments were conducted in triplicate. The analysis of each ThT trace was performed according to the equation: $dF/dt = kF(F_{lim}-F)$.[26,30]

Electron microscopy: Aβ samples (0.2 mg mL^{-1}, pH 7.4 buffered with 25 mM HEPES) were incubated at 37 °C with gentle stirring. After 24 h of incubation, samples were deposited onto carbon-coated copper mesh grids and negatively stained with 2% (w/v) uranyl acetate. The samples were examined using a Philips CM 120 BioTwin transmission electron microscope (Philips Inc. Eindhoven, The Netherlands).

Cell culture, inhibitor treatment and Aβ-immunoprecipitation: Cultivation of transfected SH-SY5Y cells overexpressing human wild-type APP695 with an amino-terminal Myc tag and a carboxy-terminal Flag tag and treatment with a prototypic tripartite BACE1 inhibitor (compound **8g** in ref. [32a]) were described previously.[32a] After 72 h of treatment with 100 nM of tripartite inhibitor or 0.1% DMSO (vehicle control), the conditioned media were collected and the Aβ peptides immunoprecipitated as described previously.[18,32a] A volume of 800 μL of cell-culture supernatant was mixed briefly with 200 μL of a 5X IP-detergent buffer (250 mM HEPES/NaOH, pH 7.4), 750 mM NaCl, 2.5% (v/v) Nonidet P-40 (Igepal CA630), 1.25% (w/v) sodium deoxycholate, 0.25% (w/v) SDS) and incubated overnight at 4 °C under rotation with 25 μL of magnetic beads (magnetic sheep-anti-mouse-IgG Dynabeads M-280 from Life Technologies, precoated with monoclonal anti-Aβ antibody 6E10, Covance). The immobilized immune complexes were collected on a magnetic stand and washed 2×5 min with PBS, 2×5 min with 50 mM NH_4HCO_3 and once with ultrapure H_2O. For MALDI-MS analysis the immunoprecipitated Aβ peptides were eluted for 5 min in 50 μL of 0.1% HCHO/0.05% n-octyl β-D-glucopyranoside (OGP) at RT.

Mass spectrometry: The masses of the intact Aβ peptides were determined as described previously.[18] In a vacuum centrifuge, the volume of the eluted fraction from immunoprecipitation was reduced to about 10 μL and 0.3 μL were spotted onto an Anchor-Chip target (Bruker Daltonics, Bremen, Germany) precoated with 2-cyano-4-hydroxycinnamic acid. After drying, the samples were washed twice with $(NH_4)H_2PO_4$ (10 mM in 0.1% TFA) and analyzed by mass spectrometry using an Ultraflex MALDI TOF/TOF instrument (Bruker Daltonics, Bremen, Germany) as described previously.[13,18]

Isoelectric point determination by the CIEF-Immunoassay: The isoelectric point (pI) of the peptide $A\beta_{-3-40}$ (**2**) was compared to those of $A\beta_{1-40}$ and $A\beta_{2-40}$ (Ana Spec Inc., Fremont CA) by capillary isoelectric-focusing immunoassay (CIEF immunoassay) on a Nano-Pro 1000 device (Protein Simple) according to a reported procedure.[18] The immunological detection shown in Figure 7 was achieved with monoclonal anti-Aβ antibody WO-2 (Millipore) with a 1:50 dilution in combination with biotinylated goat-anti-mouse

secondary antibody (1:100) and streptavidin-coupled horseradish peroxidase (1:100) (Protein Simple).

Acknowledgements

We are grateful to Dr. A. Shevchenko (MPI-GBG, Dresden) for the measurement of the high resolution ESI mass spectra and Dr. Dietmar Riedel (MPI-BPC, Göttingen) for measurement of the electron micrographs. Furthermore, we thank Christin Hafermann and Thomas Liepold for expert technical assistance. This work was supported by the German Bundesministerium für Bildung und Forschung (grant 01ED1203A) within the BIOMARKAPD project of the JPND program and by the BioPharma-Neuroallianz (grant 161A120B).

Keywords: aggregation · Alzheimer's disease · biomarkers · biophysical characterization · solid-phase peptide synthesis

[1] a) C. L. Masters, G. Simms, N. A. Weinman, G. Multhaup, B. L. McDonald, K. Beyreuther, *Proc. Natl. Acad. Sci. USA* **1985**, *82*, 4245; b) J. Hardy, D. J. Selkoe, *Science* **2002**, *297*, 353.

[2] M. Goedert, M. G. Spillantini, *Science* **2006**, *314*, 777.

[3] F. S. Esch, P. S. Keim, E. C. Beattie, R. W. Blacher, A. R. Culwell, T. Oltersdorf, D. McClure, P. J. Ward, *Science* **1990**, *248*, 1122.

[4] S. S. Sisodia, E. H. Koo, K. Beyreuther, A. Unterbeck, D. L. Price, *Science* **1990**, *248*, 492.

[5] M. Willem, S. Tahirovic, M. A. Busche, S. V. Ovsepian, M. Chafai, S. Kootar, D. Hornburg, L. D. Evans, S. Moore, A. Daria, H. Hampel, V. Müller, C. Giudici, B. Nuscher, A. Wenninger-Weinzierl, E. Kremmer, M. T. Heneka, D. R. Thal, V. Giedraitis, L. Lannfelt, U. Müller, F. J. Livesey, F. Meissner, J. Herms, A. Konnerth, H. Marie, C. Haass, *Nature* **2015**, *526*, 443.

[6] Z. Zhang, M. Song, X. Liu, S. Su Kang, D. M. Duong, N. T. Seyfried, X. Cao, L. Cheng, Y. E. Sun, S. Ping Yu, J. Jia, A. I. Levey, K. Ye, *Nat. Commun.* **2015**, *6*, 8762.

[7] T. A. Bayer, O. Wirths, *Acta Neuropathol.* **2014**, *127*, 787.

[8] J. M. Maler, H. W. Klafki, S. Paul, P. Spitzer, T. W. Groemer, A. W. Henkel, H. Esselmann, P. Lewczuk, J. Kornhuber, J. Wiltfang, *Proteomics* **2007**, *7*, 3815.

[9] J. Wiltfang, H. Esselmann, M. Bibl, A. Smirnov, M. Otto, S. Paul, B. Schmidt, H. W. Klafki, M. Maler, T. Dyrks, M. Bienert, M. Beyermann, E. Ruther, J. Kornhuber, *J. Neurochem.* **2002**, *81*, 481.

[10] D. L. Miller, I. A. Papayannopoulos, J. Styles, S. A. Bobin, Y. Y. Lin, K. Biemann, K. Iqbal, *Arch. Biochem. Biophys.* **1993**, *301*, 41.

[11] A. E. Roher, J. D. Lowenson, S. Clarke, C. Wolkow, R. Wang, R. J. Cotter, I. M. Reardon, H. A. Zürcher-Neely, R. L. Heinrikson, M. J. Ball, B. D. Greeberg, *J. Biol. Chem.* **1993**, *268*, 3072.

[12] T. C. Saido, T. Iwatsubo, D. M. Mann, H. Shimada, Y. Ihara, S. Kawashima, *Neuron* **1995**, *14*, 457.

[13] H. Schieb, H. Kratzin, O. Jahn, W. Möbius, S. Rabe, M. Staufenbiel, J. Wiltfang, H. W. Klafki, *J. Biol. Chem.* **2011**, *286*, 33747.

[14] a) C. R. Jack Jr. , M. S. Albert, D. S. Knopman, G. M. McKhann, R. A. Sperling, M. C. Carrillo, B. Thies, C. H. Phelps, *Alzheimer's Dementia* **2011**, *7*, 257; b) H. Rosenmann, *J. Mol. Neurosci.* **2012**, *47*, 1; c) N. Mattsson, I. Zegers, U. Andreasson, M. Bjerke, M. A. Blankenstein, R. Bowser, M. C. Carrillo, J. Gobom, T. Heath, R. Jenkins, A. Jeromin, J. Kaplow, D. Kidd, O. F. Laterza, A. Lockhart, M. P. Lunn, R. L. Martone, K. Mills, J. Pannee, M. Ratcliffe, L. M. Shaw, A. J. Simon, H. Soares, C. E. Teunissen, M. M. Verbeek, R. M. Umek, H. Vanderstichele, H. Zetterberg, K. Blennow, E. Portelius, *Biomarkers Med.* **2012**, *6*, 409.

[15] a) N. Kaneko, R. Yamamoto, T.-A. Sato, K. Tanaka, *Proc. Jpn. Acad. Ser. B* **2014**, *90*, 104; b) N. Kaneko, A. Nakamura, Y. Washimi, T. Kato, T. Sakurai, Y. Arahata, M. Bundo, A. Takeda, S. Niida, K. Ito, K. Toba, K. Tanaka, K. Yanagisawa, *Proc. Jpn. Acad. Ser. B* **2014**, *90*, 353.

[16] E. Portelius, M. Olsson, G. Brinkmalm, U. Rüetschi, N. Mattsson, U. Andreasson, J. Gobom, A. Brinkmalm, M. Hölttä, K. Blennow, H. Zetterberg, *J. Alzheimers Dis.* **2013**, *33*, 85.

[17] a) T. Inui, J. Bódi, H. Nishio, Y. Nishiuchi, T. Kimura, *Lett. Pept. Sci.* **2002**, *8*, 319; b) F. García-Martín, M. Quintanar-Audelo, Y. García-Ramos, L. J. Cruz, C. Gravel, R. Furic, S. Côté, J. Tulla-Puche, F. Albericio, *J. Comb. Chem.* **2006**, *8*, 213; c) L. A. Carpino, E. Krause, D. C. Sferdean, M. Schümann, H. Fabian, M. Bienert, M. Beyermann, *Tetrahedron Lett.* **2004**, *45*, 7519; d) Y. Sohma, Y. Hayashi, M. Kimura, Y. Chiyomori, A. Taniguchi, M. Sasaki, T. Kimura, Y. Kiso, *J. Pept. Sci.* **2005**, *11*, 441; e) Y. Sohma, Y. Kiso, *ChemBioChem* **2006**, *7*, 1549.

[18] U. Haußmann, O. Jahn, P. Linning, C. Janßen, T. Liepold, E. Portelius, H. Zetterberg, C. Bauer, J. Schuchardt, H.-J. Knölker, H. Klafki, J. Wiltfang, *Anal. Chem.* **2013**, *85*, 8142.

[19] M. Paradís-Bas, J. Tulla-Puche, F. Albericio, *Chem. Soc. Rev.* **2016**, *45*, 631.

[20] E. K. Tiburu, P. C. Dave, J. F. Vanlerberghe, T. B. Cardon, R. E. Minto, G. A. Lorigan, *Anal. Biochem.* **2003**, *318*, 146.

[21] G. Zheng, T. Stait-Gardner, P. G. A. Kumar, A. M. Torres, W. S. Price, *J. Magn. Reson.* **2008**, *191*, 159.

[22] D. K. Wilkins, S. B. Grimshaw, V. Receveur, C. M. Dobson, J. A. Jones, L. J. Smith, *Biochemistry* **1999**, *38*, 16424.

[23] R. Riek, P. Güntert, H. Döbeli, B. Wipf, K. Wüthrich, *Eur. J. Biochem.* **2001**, *268*, 5930.

[24] D. S. Wishart, B. D. Sykes, F. M. Richards, *J. Mol. Biol.* **1991**, *222*, 311.

[25] a) N. Rezaei-Ghaleh, K. Giller, S. Becker, M. Zweckstetter, *Biophys. J.* **2011**, *101*, 1202; b) A. Abelein, J. P. Abrahams, J. Danielsson, A. Gräslund, J. Jarvet, J. Luo, A. Tiiman, S. K. Wärmländer, *J. Biol. Inorg. Chem.* **2014**, *19*, 623.

[26] S. Kumar, N. Rezaei-Ghaleh, D. Terwel, D. R. Thal, M. Richard, M. Hoch, J. M. McDonald, U. Wüllner, K. Glebov, M. T. Heneka, D. M. Walsh, M. Zweckstetter, J. Walter, *EMBO J.* **2011**, *30*, 2255.

[27] C. Haupt, J. Leppert, R. Rönicke, J. Meinhardt, J. K. Yadav, R. Ramachandran, O. Ohlenschläger, K. G. Reymann, M. Görlach, M. Fändrich, *Angew. Chem. Int. Ed.* **2012**, *51*, 1576; *Angew. Chem.* **2012**, *124*, 1608.

[28] N. Rezaei-Ghaleh, M. Amininasab, K. Giller, S. Kumar, A. Stündl, A. Schneider, S. Becker, J. Walter, M. Zweckstetter, *J. Am. Chem. Soc.* **2014**, *136*, 4913.

[29] a) P. S. Vassar, C. F. A. Culling, *Arch. Pathol.* **1959**, *68*, 487; b) R. Khurana, C. Coleman, C. Ionescu-Zanetti, S. A. Carter, V. Krishna, R. K. Grover, R. Roy, S. Singh, *J. Struct. Biol.* **2005**, *151*, 229.

[30] H. Naiki, F. Gejyo, *Methods Enzymol.* **1999**, *309*, 305.

[31] O. Szczepankiewicz, B. Linse, G. Meisl, E. Thulin, B. Frohm, C. S. Frigerio, M. T. Colvin, A. C. Jacavone, R. G. Griffin, T. Knowles, D. M. Walsh, S. Linse, *J. Am. Chem. Soc.* **2015**, *137*, 14673.

[32] a) H. Schieb, S. Weidlich, G. Schlechtingen, P. Linning, G. Jennings, M. Gruner, J. Wiltfang, H.-W. Klafki, H.-J. Knölker, *Chem. Eur. J.* **2010**, *16*, 14412; b) P. Linning, U. Haussmann, I. Beyer, S. Weidlich, H. Schieb, J. Wiltfang, H.-W. Klafki, H.-J. Knölker, *Org. Biomol. Chem.* **2012**, *10*, 8216.

[33] K. Takeda, W. Araki, H. Akiyama, T. Tabira, *FASEB J.* **2004**, *18*, 1755.

[34] N. Mattsson, L. Rajendran, H. Zetterberg, M. Gustavsson, U. Andreasson, M. Olsson, G. Brinkmalm, J. Lundkvist, L. H. Jacobson, L. Perrot, U. Neumann, H. Borghys, M. Mercken, D. Dhuyvetter, F. Jeppsson, K. Blennow, E. Portelius, *PLoS One* **2012**, *7*, e31084.

[35] T. J. Oberstein, P. Spitzer, H.-W. Klafki, P. Linning, F. Neff, H.-J. Knölker, P. Lewczuk, J. Wiltfang, J. Kornhuber, J. M. Maler, *Neurobiol. Dis.* **2015**, *73*, 24.

[36] B. Blankemeyer-Menge, M. Nimtz, R. Frank, *Tetrahedron Lett.* **1990**, *31*, 1701.

[37] L. Hou, H. Shao, Y. Zhang, H. Li, N. K. Menon, E. B. Neuhaus, J. M. Brewer, I.-J. L. Byeon, D. G. Ray, M. P. Vitek, T. Iwashita, R. A. Makula, A. B. Przybyla, M. G. Zagorski, *J. Am. Chem. Soc.* **2004**, *126*, 1992.

Received: February 25, 2016
Published online on May 11, 2016

